Heliyon 9 (2023) e17615

Contents lists available at ScienceDirect

Heliyon

journal homepage: www.cell.com/heliyon

The utility of arterial spin labelled perfusion-weighted magnetic resonance imaging in measuring the vascularity of high grade gliomas – A prospective study

Gurkirat Chatha [a], Tarundeep Dhaliwal [a,*], Mendel David Castle-Kirszbaum [a,d], Shalini Amukotuwa [b], Leon Lai [a,d], Edward Kwan [c]

[a] Department of Neurosurgery, Monash Health, Melbourne, Australia
[b] Department of Neuroradiology, Monash Health, Melbourne, Australia
[c] Department of Pathology, Monash Health, Melbourne, Australia
[d] Department of Surgery, Monash University, Melbourne, Australia

ARTICLE INFO

Keywords:
Magnetic resonance imaging (MRI)
Cerebral blood flow (CBF)
Cerebral blood volume (CBV)
Dynamic susceptibility contrast (DSC)
Perfusion weighted imaging (PWI)
Arterial spin labelling (ASL)
Glioma

ABSTRACT

Background: Dynamic susceptibility contrast (DSC) perfusion weighted imaging (PWI) currently remains the gold standard technique for measuring cerebral perfusion in glioma diagnosis and surveillance. Arterial spin labelling (ASL) PWI is a non-invasive alternative that does not require gadolinium contrast administration, although it is yet to be applied in widespread clinical practice. This study aims to assess the utility of measuring signal intensity in ASL PWI in predicting glioma vascularity by measuring maximal tumour signal intensity in patients based on pre-operative imaging and comparing this to maximal vessel density on histopathology.

Methods: Pseudocontinuous ASL (pCASL) and DSC images were acquired pre-operatively in 21 patients with high grade gliomas. The maximal signal intensity within the gliomas over a region of interest of 100 mm^2 was measured and also normalised to the contralateral cerebral cortex (nTBF-C), and cerebellum (nTBF-Cb). Maximal vessel density per 1 mm^2 was determined on histopathology using CD31 and CD34 immunostaining on all participants.

Results: Using ASL, statistically significant correlation was observed between maximal signal intensity ($p < 0.05$) and nTBF-C ($p < 0.05$) to maximal vessel density based on histopathology. Although a positive trend was also observed nTBF-Cb, this did not reach statistical significance. Using DSC, no statistically significant correlation was found between signal intensity, nTBF-C and nTBF-Cb. There was no correlation between maximal signal intensity between ASL and DSC. Average vessel density did not correlate with age, sex, previous treatment, or IDH status.

Conclusions: ASL PWI imaging is a reliable marker of evaluating the vascularity of high grade gliomas and may be used as an adjunct to DSC PWI.

1. Introduction

High grade gliomas require a substantial blood supply to facilitate their rapid growth. Tumour vascularity is thus an important predictor of tumour grade [1], and can be assessed preoperatively using perfusion weighted imaging (PWI). Dynamic susceptibility

* Corresponding author. Department of Neurosurgery Monash Medical Centre 246 Clayton Rd, Clayton Vic 3168 Australia.
E-mail address: tarun_d5@hotmail.com (T. Dhaliwal).

https://doi.org/10.1016/j.heliyon.2023.e17615
Received 28 November 2022; Received in revised form 13 April 2023; Accepted 22 June 2023
Available online 3 July 2023

contrast (DSC) MRI is a well validated PWI technique for measuring tumour blood flow (TBF) [1,2], but necessitates the use of gadolinium contrast. Although rare, gadolinium is associated with a small risk of nephrogenic systemic fibrosis, deposition in neural structures such as the dentate nucleus and globus pallidus, local tissue reactions from contrast extravasation and hypersensitivity reactions including anaphylaxis [3]. These risks can accumulate over the course of a patient's treatment, which often involves frequent radiological surveillance. Additionally, repeated line insertions to obtain contrast imaging can be cumbersome in the paediatric population.

Arterial Spin Labelling (ASL) is an alternative perfusion weighted MR pulse sequence that does not require exogenous contrast. ASL perfusion measurements have been validated in cerebrovascular diseases [4–6], neurodegenerative diseases [7,8] and temporal lobe epilepsy [9,10]. Its application in neuro-oncology has been somewhat limited, but the results thus far in tumour diagnosis and follow-up are promising.

ASL perfusion relies on obtaining images using the protons within water molecules in arterial blood as an endogenous tracer [11]. A radiofrequency pulse is delivered to invert the magnetisation of these protons, typically at the level of the cervicomedullary junction. An image is acquired down-stream at the level of the tissue of interest. After a short delay, a second control image is acquired with unlabelled protons in the water molecules traversing the vasculature in the relaxed phase. The difference between the control and labelled signals provides a perfusion-weighted image. From this, quantitative assessment of the cerebral blood flow can be determined.

The principle of ASL PWI was developed in the early 1990s but a major limitation was poor image quality. Hence, DSC PWI has been used as a better radiological marker of tumour vascularity. Modern 3T MRI machines have improved pulse sequences and multichannel receiver array coils, and higher signal to noise ratio. Additionally, more efficient labelling with pCASL compared to PASL and CASL and more efficient imaging readouts. Has led to substantial improvements in ASL image quality leading to greater interest in this technique. ASL PWI eliminates the risks and disadvantages associated with gadolinium, and therefore may represent a safer PWI alternative for patients harbouring malignant gliomas.

The majority of studies thus far on ASL PWI in gliomas have correlated CBF to tumour grade. Although this is the most definitive means of assessing the relationship between the two, ASL is a relatively new perfusion sequence that is not readily available in many institutions. Even so, depending on the MRI scanner and software, it can be difficult and time consuming to obtain absolute CBF values. Although measuring signal intensity is a more simple technique of evaluating perfusion, it is easy to perform on a day to day basis, particularly for Neurosurgeons who do not have the access or skills to navigate the MRI software. In this study, our objective was to assess the accuracy of visual inspection of signal intensity and correlate it with vascularity on histopathology.

The aim of this study is to assess glioma perfusion by evaluating the relationship of signal intensity as measured by ASL compared to vessel density demonstrated on histopathology. We also performed a similar analysis using DSC and compared this to ASL. A discussion and comparison to DSC PWI will then follow to evaluate the clinical utility of ASL PWI in predicting glioma vascularity.

2. Materials and methods

A prospective single centre study was conducted at Monash Medical Centre, Melbourne under institutional ethics approval (HREC 59825). Patients admitted with a suspected high grade glioma were enrolled with informed consent. Inclusion criteria included: 1) adult patients aged 18 years and above; 2) intrinsic brain tumour with imaging characteristics of a glioma; 3) confirmed diagnosis of grade 4 astrocytoma or glioblastoma on histopathology. All patients underwent diagnostic and stereotactic MRI prior to surgery, as well as ASL PWI. All patients then proceeded to undergo either a stereotactic biopsy or tumour resection (either subtotal or total). See Fig. 7 for a summary of the workflow process.

2.1. Imaging protocol

All structural and perfusion sequences were obtained using a 3T MRI, Siemens Magneton Vida-XQ. Imaging sequences included ASL, DSC, T1-weight imaging, T2-weighted imaging, fluid-attenuated inversion recovery images (FLAIR) and contrast-enhanced (CE) T1-weighted imaging. The contrast agent used was 5.586g of gadoteric acid in 20 mL (Dotarem, Guerbet, Villepinte, France).

Three dimensional (3D) ASL imaging was acquired using pseudo-continuous ASL (pCASL) labelling, with a labelling duration of 1800 ms and post labelling delay of 1800 ms. This was the standard MRI protocol set by the radiology department at our institution. Additionally, these settings were based off the recommendations from Alsop et al. who suggested using 1800 ms for healthy patients less than 70 years old [12]. The mean age in our cohort was 60.6 years, with only 2 patients above the age of 70. None of our patients were comorbid from a vasculopathy point of view, so we did not expect significantly prolonged arterial transit times. A total of 14 axial sections were acquired with a 1.5 mm intersection gap. A single shot gradient echo EPI technique was used (TR/TE = 2500/11 ms, FOV = 240 × 240 mm, voxel size = 1.9 × 1.9 × 4.0 mm, bandwidth = 2232 Hz/Px, phase oversampling = 10%, number of averages = 1). The inversion and saturation times were 700 ms and 1600 ms, respectively.

DSC imaging was performed during the first pass of the contrast agent at a flow rate of 5.0 mL/s, using a single shot-shot gradient-recalled echo-planar imaging (EPI). Paramaters included a TR/TE = 1560/30 ms, flip angle of 60^{o}, FOV 220 × 220 mm, voxel size = 1.7 × 1.7 × 5.0 mm, and matrix of 128 × 128, and signal bandwidth 1,446 Hz/Px. A total of 18 axial perfusion slices were reconstructed. Post-imaging analysis was performed using syngo.MR Neuro Perfusion Engine (Siemens Healthineers, Erlangen, Germany). The arterial input function (AIF) was automatically computed, and the corresponding attenuation time curves that demonstrated a rapid increase in attenuation with sharp peaks were used for analysis. The relative cerebral blood volume (rCBV) maps were generated using voxel-wise division of the area under the concentration-time curve by the area under the AIF.

2.2. Measurement of tumour vascularity on MRI

On ASL PWI, a 100 mm^2 region of interest (ROI) was defined within the primary brain lesion that demonstrated the area of greatest signal intensity on visual inspection (Fig. 1a). The ASL perfusion images were merged with the T1 post contrast volumetric scans and used for stereotaxy. This area was the target for all stereotactic biopsies. For tumour resections, stealth navigation was used to take tumour samples from the region of highest signal intensity, alongside standard specimens for histological assessment.

The signal intensity was then compared to that within 1) the contralateral temporo-parietal cortex (Fig. 1b); and 2) contralateral cerebellar hemisphere (Fig. 1c). The ratio of greatest signal intensity of the tumour to these contralateral controls produced normalised measures of relative tumour blood flow (nTBF) to the contralateral hemisphere (nTBF-C) and cerebellum (nTBF-Cb). In a similar fashion, the same ROI within the tumour was evaluated on the DSC perfusion maps and compared to the contralateral temporal grey matter and cerebellar hemisphere (Fig. 2).

Normalised values were tested to account for age related changes in the cerebral vasculature, which are frequently observed [13, 14]. These parameters were similarly used in previous studies investigating the role of ASL PWI in predicting glioma grade. Maximal areas of cerebral perfusion were used in ROI assessments as this was thought to represent a more reliable indicator of overall glioma vascularity, based on the findings of wolf et al. [15]. Co-registration was not performed. The measurements were carefully determined by two independent authors (GC and TD).

2.3. Histopathology evaluations

The gold-standard measure of tumour vascularity was determined on histology with immunostaining for CD-31 and CD-34 (vascular endothelial cell markers). Samples from the region of maximal signal intensity on ASL were taken with the aid of stealth neuronavigation and were examined for vascularity. Immunostained slides were then examined field by field by a single pathologist at a magnification of x200 to identify the area with the highest vessel lumina. The magnification was then changed to x400 to determine the number of vessels per square millimeter within this region. Isolated endothelial cells, with or without a lumen that was clearly separated from other microvessels, were considered individual vessels. In this way, maximal vessel density was determined.

2.4. Statistical methods

Statistical analysis was performed using Prism (Graphpad, California). Normality has determined using the D'Agostino-Pearson K2 test. A Spearman correlation coefficient was used to analyse the relationship between maximal tumour signal intensity, nTBF-C and nTBF-Cb to vessel density on histology. The Mann-Whitney *U* test was used to compare vessel density and signal intensity across demographics. Multiple linear regression was then used to determine factors influencing vessel density on histology.

3. Results

A total of 21 patients were enrolled (Table 1). Mean age was 60.6 (±SD 13.1) and there was a male predominance (15/21, 73.9%). There were two cases of recurrent tumours (9.5%), while most were treatment naïve. The majority (90.5%) of cases were IDH wild type glioblastoma, while there were two (9.5%) IDH mutant Grade 4 Astrocytoma.

Average vessel density was 98.2 ± 68.5 per mm^2. There was no difference in mean vessel density between male (113.7 ± 75.2) and female (59.2 ± 20.5) patients ($p = 0.06$); nor between treatment naïve (98.8 ± 70.7) and recurrent (92.0 ± 62.2) tumours ($p = 0.95$). Average vessel density did not differ between IDH wild type (100.8 ± 71.3) and IDH mutant tumours (73.0 ± 31.1) ($p = 0.86$).

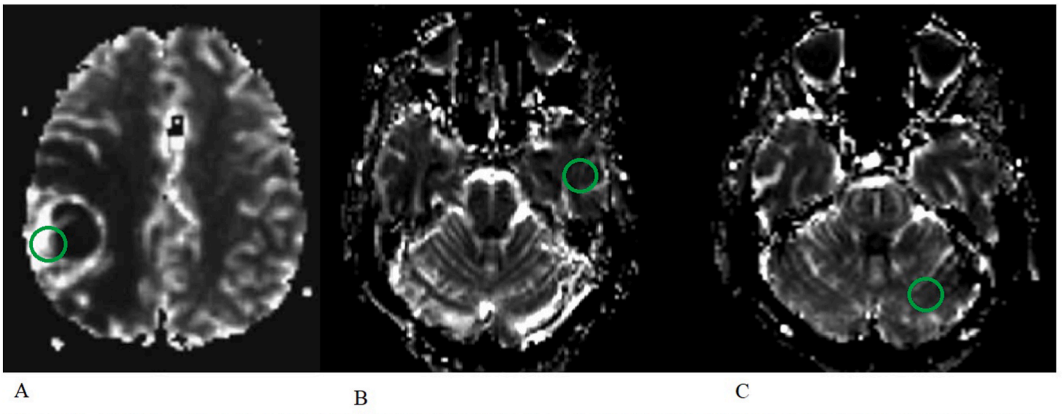

Fig. 1. A) ASL sequence measuring signal intensity over an area of 100 mm^2 in a patient with a right parietal GBM; B) ASL sequence measuring signal intensity over 100 mm^2 in the contralateral temporal grey matter cortex in the same patient; C) ASL sequence measuring signal intensity over an area of 100 mm^2 in the contralateral cerebellar hemisphere in the same patient.

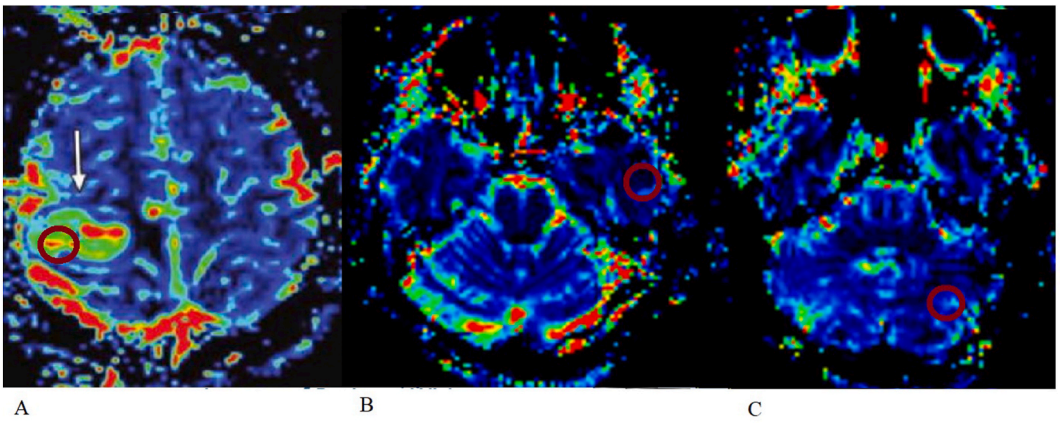

Fig. 2. A) DSC sequence measuring signal intensity over an area of 100 mm^2 in a patient with a right parietal GBM; B) DSC sequence measuring signal intensity over 100 mm^2 in the contralateral temporal grey matter cortex in the same patient; C) DSC sequence measuring signal intensity over an area of 100 mm^2 in the contralateral cerebellar hemisphere in the same patient.

Table 1
Patient demographics and histology.

Participants	N (%)
Sex	
Male	15 (71.4)
Female	6 (28.6)
Age	Mean 60.6 (SD 13.1) (Range 30–81)
Previous surgery	
First presentation	19 (90.5)
Recurrence	2 (9.5)
Histology	
IDH Wild type Glioblastoma	19 (90.5)
IDH Mutant Grade 4 Astrocytoma	2 (9.5)

Maximal signal intensity using ASL ranged from 100.9 to 1535.0. Maximal signal intensity was greater in male patients (726.8 ± 357.5 vs 375.6 ± 177.4, $p = 0.02$), but did not differ between treatment naïve (663.1 ± 345.1) and recurrent (278.4 ± 251.0) tumours ($p = 0.15$). Maximal signal intensity did not differ between IDH wild type (642.3 ± 366.6) and IDH mutant tumours (475.8 ± 73.5) ($p = 0.47$).

Maximal signal intensity using DSC ranged from 60.98 to 706.93. Maximal signal intensity did not differ between males (287.4 ± 115.5) and females (279.8 ± 242.8) ($p = 0.52$), nor did it differ between treatment naïve (300.7 ± 153.1) and recurrent (138.2 ± 109.2) tumours ($p = 0.19$). Maximal signal intensity did not differ between IDH wild type (425.1 ± 398.6) and IDH mutant tumours (270.5 ± 124.7) ($p = 0.77$).

Using ASL, tumour blood flow (nTBF) normalised to contralateral hemisphere blood flow ranged from 0.35 to 7.23 fold (mean

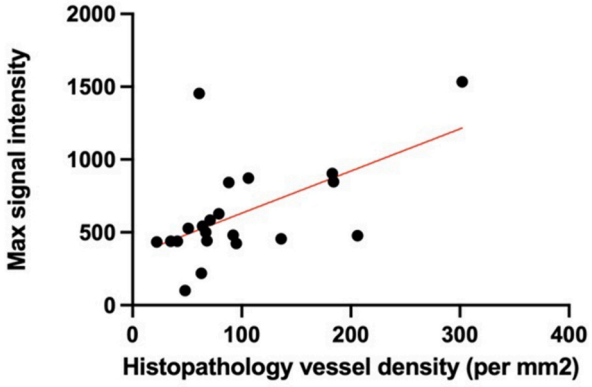

Fig. 3. Scatter plot values of maximal average signal intensity using ASL PWI compared to vessel density on histopathology. Linear regression analysis also revealed a statistically significant positive correlation ($r = 0.52$, $p = 0.02$).

2.1x), while nTBF normalised to contralateral cerebellum blood flow ranged from 0.53 to 13.54 fold (mean 3.74x). In all patients, the nTBF-Cb was greater than nTBF-C.

Using DSC, tumour blood flow (nTBF) normalised to contralateral hemisphere blood flow ranged from 0.81 to 14.74 fold (mean 2.5x), while nTBF normalised to contralateral cerebellum blood flow ranged from 1.23 to 26.38 fold (mean 3.9x). In all patients, the nTBF-Cb was greater than nTBF-C.

Maximal tumour signal intensity on ASL was directly associated with average vessel density on histopathology ($r = 0.52$, $p = 0.02$) (Fig. 3). Similarly, nTBF-C was also directly associated with average vessel density on histopathology ($r = 0.44$, $p = 0.04$) (Fig. 4). Although positively correlated, nTBF-Cb failed to reach a significant correlation with average vessel density ($r = 0.40$, $p = 0.07$).

On DSC, maximal tumour signal intensity was not associated with average vessel density on histopathology ($r = -0.31$, $p = 0.17$) (Fig. 5). Using DSC, both nTBF-C ($r = -0.19$, $p = 0.39$ and nTBF-Cb ($r = -0.35$. $p = 0.11$) failed to reach a significant correlation with average vessel density. Maximal tumour signal intensity on ASL and DSC did not correlate ($r = 0.30$, $p = 0.17$) (Fig. 6).

Multiple linear regression demonstrated that average vessel density on histopathology correlated with maximal tumour signal intensity on ASL ($p = 0.04$) but not age ($p = 0.81$), sex ($p = 0.68$), previous treatment ($p = 0.53$), or IDH status ($p = 0.96$).

Using DSC, multiple linear regression demonstrated that average vessel density on histopathology was correlated with sex ($p = 0.02$) but not maximal tumour signal intensity ($p = 0.07$), age ($p = 0.10$), previous treatment ($p = 0.51$), or IDH status ($p = 0.09$).

4. Discussion

Preoperative radiological measures of tumour vascularity are critical for accurate diagnosis and surgical planning. ASL PWI has demonstrated discriminative capacity between low and high grade gliomas [13,16–18], and oligodendroglioma and astrocytoma within low grade glioma cohorts [19]. ASL is also comparable to DSC in differentiating glioma progression from radiation necrosis [17, 20–22]. However, our study is the first to investigate the relationship between signal intensity on ASL PWI to the histological gold-standard of tumour vascularity. Together, these findings highlight that ASL PWI can reliably predict glioma vascularity and tumour grade pre-operatively.

Maximal signal intensity on ASL PWI predicted tumour vascularity in this cohort of high grade gliomas. This relationship was maintained when signal intensity was normalised to the contralateral hemisphere and was independent on patient sex, age, treatment history, and tumour IDH status. We also sought to compare the accuracy of ASL to DSC PWI. Interestingly, maximal signal intensity on ASL did not correlate to that of DSC PWI. Furthermore, using DSC PWI, maximal signal intensity, nTBF-C and nTBF-Cb also did not correlate with vessel density. This is in contrast to others who have demonstrated high concordance between the two imaging techniques [23,24,25]. There are several potential factors contributing this. Firstly, most of these studies measured absolute values of cerebral blood volume (CBV) instead of signal intensity, and therefore is it unclear whether the latter is a validated method of assessing perfusion. Secondly, the ROI for maximal signal intensity within the tumour corresponded to the same regions for both ASL and DSC. Although on visual inspection the regional of maximal signal intensity within the tumour correlated to the same area for both, there may be slight differences between the two images. In our study we used signal intensity as a marker of vascularity on radiology as this can easily be assessed by Neurosurgeons and Oncologists on a day-to-day basis, without requiring the complex processing softwares available to radiologists. From a workflow perspective, this method was not particularly time consuming.

ASL PWI differs from DSC PWI in a number of ways. ASL PWI inherently has a low signal to noise ratio due to the small proportion of labelled protons in arterial water molecules compared to the entire magnetised field. Thus, longer acquisitions are required to generate a signal with sufficient intensity to interpret [26]. A further technicality is that ASL PWI primarily measures blood flow, and

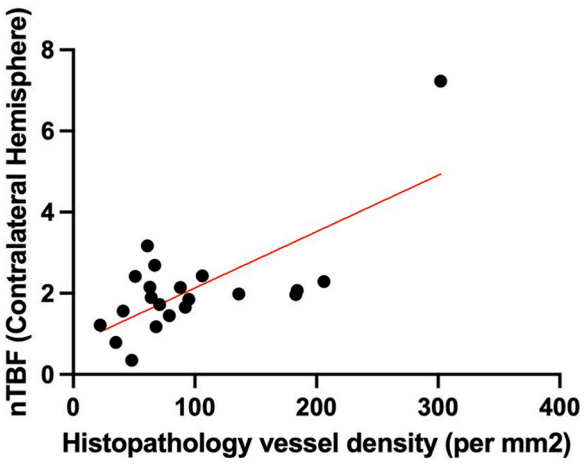

Fig. 4. Scatter plot values of nTBF-C using ASL PWI compared to vessel density on histopathology. Linear regression analysis also revealed a statistically significant positive correlation ($r = 0.44$, $p = 0.04$).

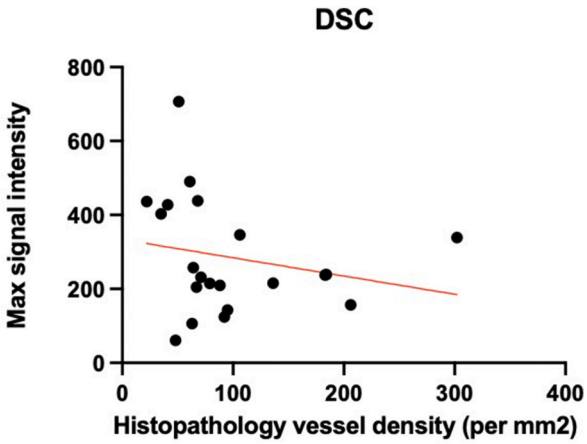

Fig. 5. Scatter plot values of average maximal signal intensity using DSC PWI compared to vessel density on histopathology. Linear regression analysis did not demonstrate a correlation (r = 0.31, p = 0.17).

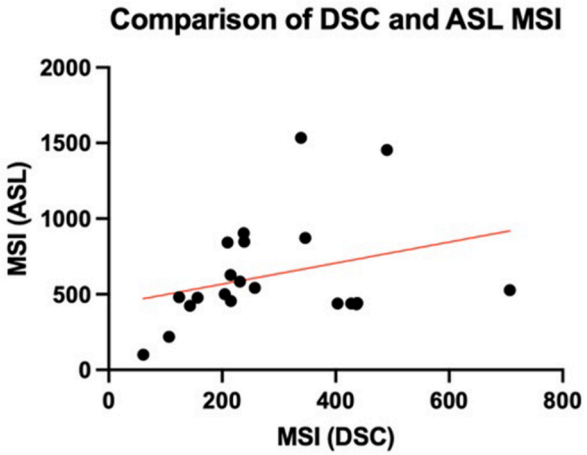

Fig. 6. Average maximal signal intensity on ASL PWI compared to DSC PWI. Linear regression analysis did not demonstrate a correlation (r = 0.30, p = 0.17).

measures of cerebral blood volume and mean transit time require additional processing and time [27–29]. Blood products or gadolinium extravasation in regions of high blood brain barrier permeability can result in susceptibility artefact in DSC PWI, leading to underestimation of CBV [30]. Water is freely diffusible across the capillary wall, and therefore changes in the blood-brain barrier permeability between tumours will not significantly impact the signal acquisition and measurements obtained using ASL PWI [13]; an important consideration in high grade glioma imaging. Thus, ASL may be more helpful than DSC in post-operative examinations where there has been significant disruption to the blood-brain barrier.

The main benefit of ASL PWI over DSC PWI is that it obviates the risks associated with line insertion and gadolinium contrast administration. The risk of adverse events related to gadolinium contrast administration, including mild reactions such as urticaria and nausea to more severe such as anaphylaxis and bronchospasm, is low, ranging between 0.1 and 4% [31]. Likewise, contrast administration is associated with a small risk of gadolinium deposition in tissue such as the dentate nucleus and globus pallidus, and an exceedingly rare risk of nephrogenic systemic fibrosis at less than 0.5% [32–34]. These risks are becoming less common with the introduction of chelating agents binding to gadolinium based contrasts, and the significance of gadolinium deposition in neural structures is unclear given that the majority of these patients remain asymptomatic. ASL PWI is an alternative in patients who have significant renal impairment, or have a gadolinium-based contrast allergy. Another advantage of ASL PWI is that absolute measurements of cerebral blood flow (ml/min/100g) can be obtained. Although possible using DSC perfusion techniques, it requires more time and post-image processing. Furthermore, blood brain barrier disruption and contrast leakage should be taken into account and adds additional complexity to this assessmeny. ASL PWI can be performed an infinite number of times, whilst with DSC PWI the number of repeated attempts is limited by the maximum contrast dose. This is more relevant for patients who have motion degraded imaging and require repeat PWI sequences. The major disadvantages of ASL PWI is that it requires more time for imaging acquisition, and the spatial resolution of the images are inferior to DSC PWI.

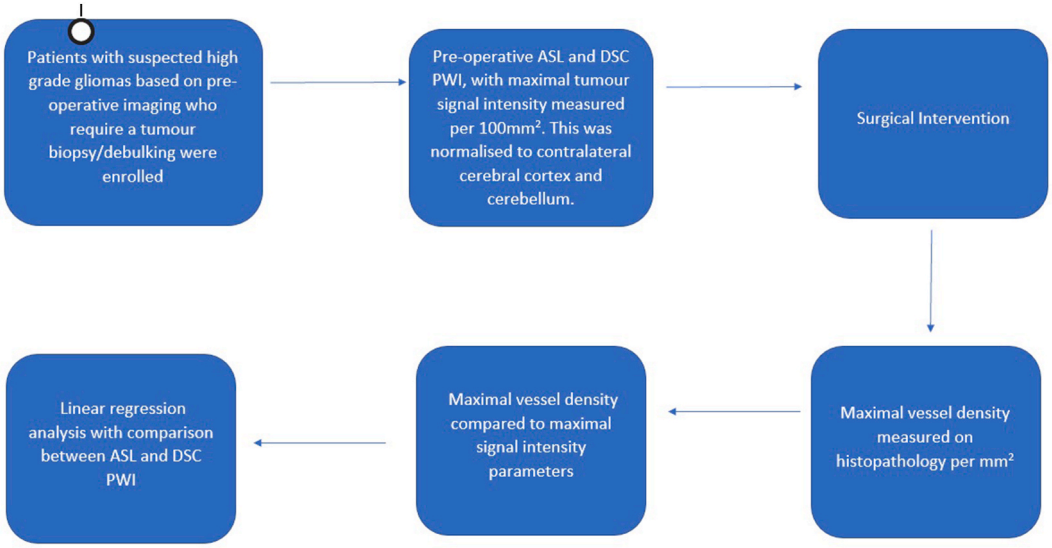

Fig. 7. Flow chart summarising workflow process for ASL and DSC analysis and comparison.

Despite the potential advantages of ASL PWI, DSC PWI should still remain the mandatory choice of perfusion weighted imaging in glioma diagnosis and follow-up. DSC is effective in differentiating between tumour progression, pseudoprogression and radiation necrosis [35–37]. ASL PWI has only been able to differentiate this in small studies. ASL PWI and DSC PWI share similar diagnostic yield in differentiating between glioma grades. A recent meta-analysis found that ASL PWI and DSC PWI have a similar pooled sensitivity (0.88 vs 0.92) and specificity (0.91 vs 0.81), respectively, in differentiating between glioma grades [38]. Despite this, gadolinium contrast administration is vital in demonstrating areas of blood-brain barrier breakdown, and therefore areas of tumour contrast enhancement. This is important overall in predicting tumour pathology, morphology and grade pre-operatively. Therefore, gadolinium-based contrast administration and DSC PWI should remain standard protocol in current MRI imaging for glioma diagnosis and surveillance. ASL PWI may be added as an adjunct until it's role and validity is clarified further.

Our study has several limitations. Small sample size limited subgroup analysis. Although maximal signal intensity and vessel density was determined carefully by visual inspection from 2 authors independently, without coregistration, this may introduce observer bias. Our cohort was uniformly comprised of high grade gliomas, and thus the utility of ASL PWI cannot necessarily be generalised to low grade glioma or non-glioma pathologies. We did not calculate CBF and CBV to correlate with histopathology as this was not possible using the imaging acquisition techniques in our study. Nevertheless, in this study, our focus was to determine the accuracy of using signal intensity as a surrogate marker of cerebral blood flow in predicting the vascularity of high grade gliomas. Using a simple grey scale approach is inherently less reliable than absolute CBF measurements. It depends on labelling efficiency, which varies from measurement to measurement due to local susceptibility and the angle of the labelling plane relative to the feeding vessel. This can lead to signal intensity differences in the left and right hemisphere. This is similarly influenced if the feeding vessels are diseased (e.g. atherosclerotic), which can render the contralateral reference inaccurate. Furthermore, grey scale depends on the arterial transit time, which could potentially change during treatment. However, the pCASL settings can be adjusted to account for this. Despite these limitations, on a practical day-to-day basis, this is a simple means of assessing perfusion by the surgical and medical teams, and the objective of this study was to assess the accuracy of this method compared to the histological gold standard.

5. Conclusions

ASL PWI discriminates vessel density in high grade gliomas, without the need for gadolinium. Maximal signal intensity did not correlate between ASL and DSC PWI, and likewise, maximal signal intensity, nTBF-C and nTBF-Cb using DSC did not correlated with vessel density on histopathology. Measuring signal intensity on a grey scale has limitations and is less reliable than using CBF. = Further studies are required to validate its utility in differentiating between low and high grade gliomas, and non-glioma brain tumours. As we endeavour toward a new era of contrast-free glioma imaging, ASL PWI will become integral to diagnostic workup and surveillance of glioma.

Author contribution statement

Gurkirat Chatha: Conceived and designed the experiments; Performed the experiments; Analyzed and interpreted the data; Contributed reagents, materials, analysis tools or data; Wrote the paper.

Tarundeep Dhaliwal: Performed the experiments; Analyzed and interpreted the data; Contributed reagents, materials, analysis tools or data; Wrote the paper.

Mendel David Castle-Kirszbaum: Analyzed and interpreted the data; Wrote the paper.
Shalini Amukotuwa: Leon Lai: Conceived and designed the experiments; Contributed reagents, materials, analysis tools or data.
Edward Kwan: Performed the experiments.

Data availability statement

Data included in article/supp. material/referenced in article.

Funding

The authors report no involvement in the research by the sponsor that could have influenced the outcome of this work.

Declaration of competing interest

The authors declare that they do not have any competing financial or other interests pertaining to this study.

References

[1] D.N. Louis, A. Perry, P. Wesseling, D.J. Brat, I.A. Cree, D. Figarella-Branger, C. Hawkins, H.K. Ng, S.M. Pfister, G. Reifenberger, R. Soffietti, A. von Deimling, D. W. Ellison, The 2021 WHO classification of tumors of the central nervous system: a summary, Neuro Oncol. 23 (8) (2021 Aug 2) 1231–1251.
[2] H.J. Aronen, I.E. Gazit, D.N. Louis, B.R. Buchbinder, F.S. Pardo, R.M. Weisskoff, G.R. Harsh, G.R. Cosgrove, E.F. Halpern, F.H. Hochberg, et al., Cerebral blood volume maps of gliomas: comparison with tumor grade and histologic findings, Radiology 191 (1) (1994 Apr) 41–51.
[3] V. Granata, M. Cascella, R. Fusco, et al., Immediate adverse reactions to gadolinium-based MR contrast media: a retrospective analysis on 10,608 examinations, BioMed Res. Int. 2016 (2016), 3918292, https://doi.org/10.1155/2016/3918292.
[4] J.A. Chalela, D.C. Alsop, J.B. Gonzalez-Atavales, et al., Magnetic resonance perfusion imaging in acute ischemic stroke using continuous arterial spin labeling, Stroke 31 (2000) 680–687.
[5] H. Kimura, H. Kado, Y. Koshimoto, et al., Multislice continuous arterial spin-labeled perfusion MRI in patients with chronic occlusive cerebrovascular disease: a correlative study with CO2 PET validation, J. Magn. Reson. Imag. 22 (2005) 189–198.
[6] J.A. Detre, D.C. Alsop, L.R. Vives, et al., Noninvasive MRI evaluation of cerebral blood flow in cerebrovascular disease, Neurology 50 (1998) 633–641.
[7] D.C. Alsop, J.A. Detre, M. Grossman, Assessment of cerebral blood flow in Alzheimer's disease by spin-labeled magnetic resonance imaging, Ann. Neurol. 47 (2000) 93–100.
[8] A.T. Du, G.H. Jahng, S. Hayasaka, et al., Hypoperfusion in frontotemporal dementia and Alzheimer disease by arterial spin labeling MRI, Neurology 67 (2006) 1215–1220.
[9] H.L. Liu, P. Kochunov, J. Hou, et al., Perfusion-weighted imaging of interictal hypoperfusion in temporal lobe epilepsy using FAIR-HASTE: comparison with H215O PET measurements, Magn. Reson. Med. 45 (2001) 431–435.
[10] H.L. Liu, P. Kochunov, J. Hou, et al., Perfusion-weighted imaging of interictal hypoperfusion in temporal lobe epilepsy using FAIR-HASTE: comparison with H215O PET measurements, Magn. Reson. Med. 45 (2001) 431–435.
[11] S. Haller, G. Zaharchuk, D.L. Thomas, K.O. Lovblad, F. Barkhof, X. Golay, Arterial spin labeling perfusion of the brain: emerging clinical applications, Radiology 281 (2) (2016 Nov) 337–356.
[12] D.C. Alsop, J.A. Detre, X. Golay, M. Günther, J. Hendrikse, L. Hernandez-Garcia, H. Lu, B.J. MacIntosh, L.M. Parkes, M. Smits, M.J. van Osch, D.J. Wang, E. C. Wong, G. Zaharchuk, Recommended implementation of arterial spin-labeled perfusion MRI for clinical applications: a consensus of the ISMRM perfusion study group and the European consortium for ASL in dementia, Magn. Reson. Med. 73 (1) (2015 Jan) 102–116.
[13] P. Clement, H.J. Mutsaerts, L. Václavů, E. Ghariq, F.B. Pizzini, M. Smits, M. Acou, J. Jovicich, et al., Variability of physiological brain perfusion in healthy subjects - a systematic review of modifiers. Considerations for multi-center ASL studies, J. Cerebr. Blood Flow Metabol. 38 (9) (2018 Sep) 1418–1437.
[14] N. Zhang, M.L. Gordon, Y. Ma, B. Chi, J.J. Gomar, S. Peng, P.B. Kingsley, D. Eidelberg, T.E. Goldberg, The age-related perfusion pattern measured with arterial spin labeling MRI in healthy subjects, Front. Aging Neurosci. 10 (2018 Jul 17) 214.
[15] R.L. Wolf, J. Wang, S. Wang, E.R. Melhem, D.M. O'Rourke, K.D. Judy, J.A. Detre, Grading of CNS neoplasms using continuous arterial spin labeled perfusion MR imaging at 3 Tesla, J. Magn. Reson. Imag. 22 (4) (2005 Oct) 475–482.
[16] J. Gaa, S. Warach, P. Wen, V. Thangaraj, P. Wielopolski, R.R. Edelman, Noninvasive perfusion imaging of human brain tumors with EPISTAR, Eur. Radiol. 6 (4) (1996) 518–522.
[17] C. Warmuth, M. Gunther, C. Zimmer, Quantification of blood flow in brain tumors: comparison of arterial spin labeling and dynamic susceptibility-weighted contrast-enhanced MR imaging, Radiology 228 (2) (2003 Aug) 523–532.
[18] M.A. Weber, S. Zoubaa, M. Schlieter, E. Jüttler, H.B. Huttner, K. Geletneky, C. Ittrich, M.P. Lichy, A. Kroll, J. Debus, F.L. Giesel, M. Hartmann, M. Essig, Diagnostic performance of spectroscopic and perfusion MRI for distinction of brain tumors, Neurology 66 (12) (2006 Jun 27) 1899–1906.
[19] Y. Ozsunar, M.E. Mullins, K. Kwong, F.H. Hochberg, C. Ament, P.W. Schaefer, R.G. Gonzalez, M.H. Lev, Glioma recurrence versus radiation necrosis? A pilot comparison of arterial spin-labeled, dynamic susceptibility contrast enhanced MRI, and FDG-PET imaging, Acad. Radiol. 17 (3) (2010 Mar) 282–290.
[20] J. Ye, S.K. Bhagat, H. Li, X. Luo, B. Wang, L. Liu, G. Yang, Differentiation between recurrent gliomas and radiation necrosis using arterial spin labeling perfusion imaging, Exp. Ther. Med. 11 (6) (2016 Jun) 2432–2436.
[21] Y. Liu, G. Chen, H. Tang, L. Hong, W. Peng, X. Zhang, Systematic review and meta-analysis of arterial spin-labeling imaging to distinguish between glioma recurrence and post-treatment radiation effect, Ann. Palliat. Med. 10 (12) (2021 Dec) 12488–12497.
[22] C. Cohen, B. Law-Ye, D. Dormont, D. Leclercq, L. Capelle, M. Sanson, et al., Pseudo-continuous arterial spin labelling shows high diagnostic performance in the detection of postoperative residual lesion in hyper-vascularised adult brain tumours, Eur. Radiol. 30 (5) (2020 May) 2809–2820.
[23] H. Järnum, E.G. Steffensen, L. Knutsson, et al., Perfusion MRI of brain tumours: a comparative study of pseudo-continuous arterial spin labelling and dynamic susceptibility contrast imaging, Neuroradiology 52 (4) (2010) 307–317.
[24] P. Lehmann, P. Monet, G. de Marco, et al., A comparative study of perfusion measurement in brain tumours at 3 Tesla MR: arterial spin labeling versus dynamic susceptibility contrast-enhanced MRI, Eur. Neurol. 64 (1) (2010) 21–26.
[25] J. Jiang, L. Zhao, Y. Zhang, S. Zhang, Y. Yao, Y. Qin, C.Y. Wang, W. Zhu, Comparative analysis of arterial spin labeling and dynamic susceptibility contrast perfusion imaging for quantitative perfusion measurements of brain tumors, Int. J. Clin. Exp. Pathol. 7 (6) (2014 May 15) 2790–2799.
[26] J.C. Ferré, E. Bannier, H. Raoult, G. Mineur, B. Carsin-Nicol, J.Y. Gauvrit, Arterial spin labeling (ASL) perfusion: techniques and clinical use, Diag. Inter.Imag. 94 (12) (2013 Dec) 1211–1223.
[27] M. Günther, M. Bock, L.R. Schad, Arterial spin labeling in combination with a look-locker sampling strategy: inflow turbo-sampling EPI-FAIR (ITS-FAIR), Magn. Reson. Med. 46 (5) (2001 Nov) 974–984.
[28] E.T. Petersen, T. Lim, X. Golay, Model-free arterial spin labeling quantification approach for perfusion MRI, Magn. Reson. Med. 55 (2006) 219–232.
[29] J. Wang, D.C. Alsop, H.K. Song, et al., Arterial transit time imaging with flow encoding arterial spin tagging (FEAST), Magn. Reson. Med. 50 (2003) 599–607.

[30] S. Nakajima, et al., Differentiation between primary central nervous system lymphoma and glioblastoma: a comparative study of parameters derived from dynamic susceptibility contrast-enhanced perfusion-weighted MRI, Clin. Radiol. 70 (12) (2015) 1393–1399.
[31] T.J. Fraum, D.R. Ludwig, M.R. Bashir, K.J. Fowler, Gadolinium-based contrast agents: a comprehensive risk assessment, J. Magn. Reson. Imag. 46 (2) (2017 Aug) 338–353.
[32] A. Spinazzi, MRI contrast agents and nephrogenic systemic fibrosis, in: F.G. Schellock, J.V. Crues, A.M. Karacozoff (Eds.), MRI Bioeffects, Safety, and Patient Management, fourth ed., Biomedical Research Publishing Group, Los Angeles, 2014, pp. 256–281.
[33] N. Schieda, P.J. Maralani, C. Hurrell, A.K. Tsampalieros, S. Hiremath, Updated clinical practice guideline on use of gadolinium-based contrast agents in kidney disease issued by the Canadian association of radiologists, Can. Assoc. Radiol. J. 70 (3) (2019 Aug) 226–232.
[34] S.A. Woolen, P.R. Shankar, J.J. Gagnier, M.P. MacEachern, L. Singer, M.S. Davenport, Risk of nephrogenic systemic fibrosis in patients with stage 4 or 5 chronic kidney disease receiving a group II gadolinium-based contrast agent: a systematic review and meta-analysis, JAMA Intern. Med. 180 (2) (2020 Feb 1) 223–230.
[35] G. Quan, K. Zhang, Y. Liu, J.L. Ren, D. Huang, W. Wang, T. Yuan, Role of dynamic susceptibility contrast perfusion MRI in glioma progression evaluation, JAMA Oncol. (2021), 1696387, 2021 Feb 9.
[36] B. Wan, S. Wang, M. Tu, B. Wu, P. Han, H. Xu, The diagnostic performance of perfusion MRI for differentiating glioma recurrence from pseudoprogression: a meta-analysis, Medicine (Baltim.) 96 (11) (2017 Mar).
[37] J.L. Boxerman, B.M. Ellingson, S. Jeyapalan, H. Elinzano, R.J. Harris, J.M. Rogg, W.B. Pope, H. Safran, Longitudinal DSC-MRI for distinguishing tumor recurrence from pseudoprogression in patients with a high-grade glioma, Am. J. Clin. Oncol. 40 (3) (2017 Jun) 228–234.
[38] J. Luan, M. Wu, X. Wang, L. Qiao, G. Guo, C. Zhang, The diagnostic value of quantitative analysis of ASL, DSC-MRI and DKI in the grading of cerebral gliomas: a meta-analysis, Radiat. Oncol. 15 (1) (2020 Aug 24) 204.